



Published in final edited form as:

J Biomed Mater Res. 1998 September 5; 41(3): 422–430.

Relative importance of surface wettability and charged functional groups on NIH 3T3 fibroblast attachment, spreading, and cytoskeletal organization

Ken Webb, Vladimir Hlady, and Patrick A. Tresco

Center for Biopolymers at Interfaces, Department of Bioengineering, 2480 Merrill Engineering Building, University of Utah, Salt Lake City, Utah 84112

Abstract

Understanding the relationships between material surface properties, adsorbed proteins, and cellular responses is essential to designing optimal material surfaces for implantation and tissue engineering. In this study, we have prepared model surfaces with different functional groups to provide a range of surface wettability and charge. The cellular responses of attachment, spreading, and cytoskeletal organization have been studied following preadsorption of these surfaces with dilute serum, specific serum proteins, and individual components of the extracellular matrix. When preadsorbed with dilute serum, cell attachment, spreading, and cytoskeletal organization were significantly greater on hydrophilic surfaces relative to hydrophobic surfaces. Among the hydrophilic surfaces, differences in charge and wettability influenced cell attachment but not cell area, shape, or cytoskeletal organization. Moderately hydrophilic surfaces (20–40 degree water contact angle) promoted the highest levels of cell attachment. Preadsorption of the model surfaces with bovine serum albumin (BSA) resulted in a pattern of cell attachment very similar to that observed following preadsorption with dilute serum, suggesting an important role for BSA in regulating cell attachment to biomaterials exposed to complex biological media.

Keywords

cell attachment; cell spreading; silane chemistry; model surfaces; cytoskeletal organization

INTRODUCTION

The ability to predict and control the interactions of cells with nonbiological materials underlies the rational design of biocompatible implants and tissue-engineered biohybrid organs. During implantation of such devices, the material surface is exposed to numerous proteins present in blood, interstitial fluid, and damaged extracellular matrix, resulting in the formation of a complex layer of adsorbed proteins at the material surface. Likewise, cell culture systems that utilize two- and three-dimensional polymeric supports for studying cell behavior in a serum- or protein-containing medium are affected by proteins adsorbed at material interfaces. Some of these proteins that are present in blood, serum, and the extracellular matrix, such as fibronectin, vitronectin, collagen, and laminin, contain specific amino acid sequences that bind to cell-surface integrin receptors and influence cell behavior and gene expression.

Correspondence to: Patrick A. Tresco.

Correspondence to: P. Tresco; e-mail: Patrick.Tresco@m.cc.utah.edu.

Integrin ligation by cells is followed by receptor aggregation and the accumulation of intracellular proteins at the integrin cytoplasmic domains, forming focal adhesions that serve to integrate the extracellular matrix with the actin cytoskeleton.¹ In addition, several signaling molecules, such as focal adhesion kinase (FAK), accumulate, become phosphorylated, and initiate signal transduction cascades that lead to the activation of transcription factors that affect gene expression. (For recent reviews see references²⁻⁴.)

Throughout the history of biomaterials development, there have been numerous empirical studies demonstrating differences in cell behavior in response to different material surface chemistries. One explanation for these differences is that material surface properties influence the composition of the adsorbed protein layer, which, in turn, regulates how cells respond to the material. Numerous studies indicate that surface wettability and charge influence the type, quantity, and conformation of adsorbed proteins on material surfaces.⁵

Polymer thin films, silanized glass, and self-assembled monolayers of alkanethiols have been used as model surfaces for studying the interactions among material surface properties, protein adsorption, and cellular responses. Several recent studies have demonstrated greater cell attachment and cell spreading on hydrophilic, positively charged amine-modified surfaces relative to hydrophobic surfaces, both in the presence and absence of serum.⁶⁻¹⁴ Similarly, other studies have demonstrated greater cell attachment to hydrophilic, negatively charged clean glass relative to hydrophobic surfaces in the presence of serum.¹⁵ Other groups have observed a maximum number of adherent cells on regions of methyl-silica gradient surfaces at moderate levels of wettability comparable to that of amine-modified surfaces.¹⁶

Currently, the relative importance of surface wettability and surface charge in influencing how cells adhere to a surface, the morphology they assume, and the cytoskeletal organization they develop remains unclear. To the best of our knowledge, no single investigation has utilized a broad range of model surface chemistries to study this interaction. Therefore, the purpose of this study was to use model surfaces with different degrees of wettability and charge to examine their influence on cell attachment, cell morphology, and cytoskeletal organization following exposure of the model surfaces to a variety of conditions, including dilute serum, specific serum proteins, and individual components of the extracellular matrix. The long-term objective of this work is to understand how material surface properties influence cellular responses at the material interface so as to develop general principles that can be used to engineer clinically useful implantable devices and tissue-engineered constructs.

MATERIALS AND METHODS

Model surface preparation

Glass microscope slides were cleaned in 30% (v/v) hydrogen peroxide in concentrated sulfuric acid for ½ h, rinsed with deionized distilled water, and dried for 1 h at 100°C. Surfaces with terminal thiol groups (so-call thiol surfaces) were prepared by immersing the clean slides in 2% (v/v) 3-mercaptopropyltrimethoxysilane (Fluka, Ronkonkoma, NY) in trichloroethylene (TCE) for 12 h, as previously described.¹⁷ The slides were rinsed with TCE and acetone, each followed by drying with filtered nitrogen gas. Oxidized thiol surfaces were prepared by exposing thiol surfaces to UV light (400 W, Model ELC 4000, Electrolite Corp.) at 15 mW/cm² for 10 min. Amine-modified glass slides were prepared by immersing clean slides in 1% (v/v) 3-aminopropyltriethoxysilane (Fluka, Ronkonkoma, NY) in toluene for 1 h. The slides were rinsed with 95% ethanol and dried with filtered nitrogen gas. Quaternary amine surfaces were prepared by placing amine-modified glass slides in 5% (v/v) methyl iodide (Fisher, Pittsburgh, PA) in absolute ethanol for 18 h. The slides were rinsed with 95% ethanol and dried with filtered nitrogen gas. Methyl-modified surfaces were prepared by immersing clean slides in 0.05% (v/v) dimethyldichlorosilane (United Chemical Technologies, Bristol, PA) in TCE

for 30 min. The surfaces were rinsed with acetone and dried for 1 h at 120°C. All modified slides were used immediately after preparation.

Surface characterization

Static water contact angles on modified glass surfaces were measured by the sessile drop method, using deionized, distilled water buffered with 1.45 mM of sodium phosphate monobasic ($\text{NaH}_2\text{PO}_4 \cdot \text{H}_2\text{O}$) and 8.1 mM of sodium phosphate dibasic (Na_2HPO_4) at pH 2.0 and 7.5 as the probe liquids. Oxidized thiol-, amine-, thiol-, and methyl-modified glass surfaces also were analyzed by X-ray photoelectron spectroscopy (XPS).

Cell culture

NIH 3T3 fibroblasts (American Type Culture Collection, CCL 92) were cultured in Dulbecco's modified Eagle's medium (DMEM, Sigma, St. Louis, MO) supplemented with 10% bovine calf serum (Hyclone, Logan, UT) and 50 U/mL of penicillin and streptomycin (Sigma, St. Louis, MO). For routine culture and all experiments, the cells were maintained at 37°C in a humidified 5% CO_2 atmosphere with fresh medium added every 2 days.

Adhesion and morphology assays

Confluent monolayers of cells were dissociated with 0.02% EDTA in phosphate-buffered saline (PBS) without divalent ions, centrifuged, and resuspended in PBS. Cells were counted with a hemacytometer and diluted to 6.8×10^4 cells/mL. The glass slides with modified surfaces were placed in 100 mm plastic petri dishes (Falcon, Becton Dickinson, Bedford, MA) and covered with 1 mL of 5% bovine calf serum, a specific protein, or PBS for protein-free experiments. For experiments in which oxidized thiol surfaces were compared with thiol chemistry, 75×25 mm glass microscope slides were used on which half of the surface had been oxidized by exposure to UV light, as previously described, while the other portion was masked to prevent oxidation. For the comparison between oxidized thiol- and amine-modified surfaces, oxidized thiol- and quaternary amine-modified surfaces, and oxidized thiol- and methyl-modified surfaces, two separate 37.5×25 mm slides were used. Each petri dish contained two distinct surface chemistries that were compared at the same seeding density. After 15 min of protein adsorption, the slides were covered with an additional 20 mL of PBS and rinsed three times with PBS, then three times with serum-free DMEM by removing 10 of the 20 mL in the dish and adding 10 mL of the rinse solution. In this manner, nonadsorbed protein was removed and the surfaces were transferred to serum-free DMEM while maintaining a minimum volume of 10 mL in the dish to prevent formation of an air/solid interface that could denature the adsorbed proteins at the surface. One mL of cell suspension was added to a final volume of 20 mL of serum-free DMEM and incubated for 30 min. The surfaces then were rinsed three times, as described above, with 10 mL of serum-free DMEM to remove nonadherent cells and incubated for an additional 24 h. After incubation, the cells were fixed with 0.1% glutaraldehyde and observed using phase-contrast microscopy. Digitized images of cells were recorded with a CCD camera and analyzed using NIH Image v 1.57 image analysis software.

Cytoskeletal staining of adherent NIH 3T3 fibroblasts on model surface

NIH 3T3 fibroblasts were seeded, as described above, on 25 mm glass coverslips (Fisher, Pittsburgh, PA) that were modified in the same manner as previously described for the glass slides and placed in serum-free DMEM. After 24 h of incubation, the cells were fixed in 3% paraformaldehyde in PBS for 10 min and permeabilized with 0.5% Triton X-100 in PBS for 2 min. The cells were stained in three separate steps with rhodamine-phalloidin (5 units/mL, Molecular Probes, Eugene, OR) for 45 min, mouse antihuman vinculin monoclonal antibody (1:100 dilution, Sigma, St. Louis, MO) for 1 h, and FITC-conjugated goat antimouse

monoclonal antibody (1:20 dilution, CalBiochem, La Jolla, CA) for 30 min. Rhodamine-phalloidin was prepared in PBS, and both antibodies were diluted in staining medium (Hank's Balanced Salt Solution without sodium bicarbonate, 5% bovine calf serum, 0.05% w/v sodium azide, and buffered to pH 7.4 with 2 mM of N-2-hydroxyethylpiperazine-N'-2-ethanesulfonic acid (HEPES, Sigma, St. Louis, MO) and 2 mM of HEPES-sodium salt (Sigma, St. Louis, MO)). Following each step, the surfaces were rinsed four times in staining medium. Once stained, the surfaces were rinsed four times in distilled water, mounted on microscope slides in 90% glycerol/10% PBS with 1 mg/mL n-propyl gallate (Sigma, St. Louis, MO), and sealed with clear nail varnish. Fluorescence micrographs were taken on a Zeiss Axioplan II microscope with a 40× objective using standard rhodamine and fluorescein filters.

Statistical analysis

For cell attachment experiments, the number of adherent cells in 35 separate viewing fields at 100× magnification was determined for each surface-modified slide, with a minimum of three separate slides or 105 viewing fields per experimental group. The area of the viewing fields analyzed was 10.8% of the total surface area for each surface-modified slide. All of the cell attachment statistical analysis was performed relative to the attachment of cells to the slides having the oxidized thiol surface modification. Cell area and cell aspect ratio measurements were performed on images of 63 cells recorded from three separate slides (21 cells/sample) of each surface modification. All data have been reported as the mean ± the standard error of the mean. The Student's *t* test was used for statistical comparisons, with $p < 0.05$ defined as significantly different.

RESULTS

Characterization of model surfaces

Static water contact angles measured by the sessile drop method on modified glass surfaces with probe liquids at pH 2.0 and pH 7.5 are listed in Table I. The atomic percent of relevant elemental chemistries as determined by XPS analysis for clean unmodified glass, oxidized thiol-, amine-, thiol-, and methyl-modified slides also are listed. High resolution XPS sulfur S2p spectra of thiol surfaces showed two peaks indicating the presence of sulfur in both reduced (164 eV) and oxidized (169 eV) states. The ratio of reduced to oxidized sulfur was 2.1 to 1. Only one S2p peak at 169 eV was present in the XPS spectra recorded for the oxidized thiol surface, indicating complete oxidation of the thiol groups.

NIH 3T3 fibroblast attachment, spreading, and cytoskeletal organization on model surfaces preadsorbed with 5% serum

The statistics of the NIH 3T3 fibroblast attachment to model surfaces preadsorbed with 5% serum is shown in Figure 1. The number of adherent cells was significantly greater on quaternary amine and amine surfaces relative to oxidized thiol surfaces. However, the number of adherent cells was significantly lower on thiol and methyl surfaces relative to oxidized thiol surfaces. In addition, cell attachment was significantly higher on quaternary amine surfaces relative to amine surfaces.

NIH 3T3 fibroblasts cultured on 5% serum preadsorbed oxidized thiol, quaternary amine, and amine surfaces for 24 h attained a well spread morphology characterized by significantly higher cell area and lower aspect ratio relative to thiol and methyl surfaces (Fig. 2). However, cell area and aspect ratio were not significantly different between oxidized thiol, quaternary amine, or amine surfaces. Cells on thiol and methyl surfaces attained a bipolar, spindle-shaped morphology characterized by low cell area and high aspect ratio. Cell area was significantly lower on methyl surfaces relative to thiol surfaces while aspect ratio was not significantly different.

The well spread morphology predominant on oxidized thiol, quaternary amine, and amine surfaces was associated with a complex network of actin stress fibers and numerous focal adhesions (Fig. 3). The bipolar, spindle-shaped cells on thiol and methyl surfaces displayed less prominent actin stress fibers that appeared to be arranged parallel to the long axis of the cell. Similarly, fewer focal adhesions were observed and these were largely restricted to one edge of the cell membrane.

NIH 3T3 fibroblast attachment to oxidized thiol/thiol-modified surfaces preadsorbed with individual proteins

Oxidized thiol/thiol surfaces were preadsorbed with individual serum proteins at concentrations comparable to that present in 5% serum or individual extracellular matrix proteins. Preadsorption with bovine serum albumin (BSA, 2.1 mg/mL) or high-density lipoprotein (HDL, 0.065 mg/mL) resulted in a significantly greater number of adherent cells on oxidized thiol surfaces relative to thiol surfaces (Fig. 4). Preadsorption of IgG (0.5 mg/mL) did not result in a significant difference in the number of adherent cells.

Preadsorption of fibronectin (FN, 20 μ g/mL) and laminin (LN, 20 μ g/mL) reversed this effect, resulting in a significantly greater number of adherent cells on thiol surfaces relative to oxidized thiol surfaces. However, preadsorption with type IV collagen (CIV, 33 μ g/mL) did not produce a significant difference in cell attachment.

NIH 3T3 fibroblast attachment to model surfaces preadsorbed with BSA

Cell attachment to model surfaces preadsorbed with 2.1 mg/mL of BSA followed a pattern similar to that produced by 5% serum preadsorption (Fig. 5). A significantly greater number of adherent cells were observed on quaternary amine and amine surfaces relative to oxidized thiol surfaces. A significantly lower number of adherent cells were observed on thiol surfaces relative to oxidized thiol surfaces. BSA preadsorbed methyl surfaces were the only experimental condition that resulted in complete elimination of cell attachment.

NIH 3T3 fibroblast attachment to model surfaces without preadsorbed protein

As a control experiment, cells also were seeded on model surfaces without any preadsorbed protein (Fig. 6). A significantly greater number of adherent cells were observed on quaternary amine and thiol surfaces relative to oxidized thiol surfaces. Cell attachment to amine and methyl surfaces was not significantly different from that to oxidized thiol surfaces.

DISCUSSION

The objective of this study was to gain insight into the relationships among material surface properties, protein adsorption, cell attachment, spreading, and cytoskeletal organization. Glass microscope slides were prepared with five different surface chemistries providing varying degrees of wettability and charge. Oxidized thiol-, quaternary amine-, and amine-modified glass surfaces with water contact angles less than 40 degrees were considered hydrophilic while thiol- and methyl-modified surfaces were considered hydrophobic. The pH dependence of the water contact angle for the amine-modified surface indicated that chargeable amine groups were present on the surface. However, the higher contact angle measurement obtained with the pH 7.5 probe liquid suggests that these surface groups were largely unprotonated under physiological conditions. The loss of pH dependence following the surface amine quaternization suggests that the amine groups had been quaternized and were charged at physiological pH. XPS analysis of the thiol surfaces indicated the presence of sulfur in both reduced (164 eV) and oxidized (169 eV) states. However, our water contact angle measurements for this surface were consistent with literature values for a thiol functionalized surface.^{17,18} We believe that the partial oxidation of the thiol surfaces occurred during

handling, transport, and preparation for XPS analysis. The single S2p binding energy peak present in the XPS spectrum of the oxidized thiol-modified surfaces at 169 eV suggests that the thiol groups were indeed fully oxidized to a sulfonate-like (SO₃H) functionality.¹⁹ However, the exact stoichiometry of the sulfur oxidation state could not be determined due to the large background O signal of the underlying SiO₂ substrate. Our results indicate that when material surfaces are exposed to dilute serum, cell attachment, spreading, and cytoskeletal organization are greater on hydrophilic surfaces relative to hydrophobic surfaces. Among the hydrophilic surfaces, differences in charge and wettability influenced cell attachment but not spreading or cytoskeletal organization. BSA, a major protein constituent of serum, promoted a pattern of cell attachment very similar to that observed with 5% serum, suggesting that this protein plays an important role in the cellular response to materials that encounter a dilute serum-containing environment.

A number of recent studies using photolithographic and UV photochemical methods have demonstrated preferential attachment of a variety of anchorage-dependent cell types to amine-modified surfaces patterned on hydrophobic backgrounds in the presence of serum.^{6,10-14} There has been considerable debate as to whether these results are attributable to the moderate surface wettability or putative positive charge of surface amine groups. In our experiments, cell attachment to quaternary amine and amine surfaces was over 500% greater than to the other three surfaces, suggesting that the moderate wettability shared by these two surfaces is the major factor promoting higher cell attachment. Using a variety of polymer thin films with different degrees of wettability, van Wachem et al. also observed maximum cell attachment in a range of surface wettability characterized by water contact angles between 20 and 60 degrees.^{20,21} Similarly, maximum cell attachment has been reported in a range of moderate surface wettability on methyl-silica gradient surfaces.¹⁶ Cell attachment to quaternary amine surfaces was 50% greater than to amine surfaces, suggesting that positively charged surface functional groups further enhance cell attachment. However, this change is relatively small compared to the overall increase in cell attachment to both moderately wettable surfaces. Our study also included a highly wettable, negatively charged oxidized thiol surface that produced a level of cell attachment intermediate between the moderately wettable amine surfaces and the hydrophobic surfaces. We were not able to determine in this study if the negatively charged functional groups or the high wettability was responsible for this effect.

Other researchers also have attached cells to amine-patterned regions on hydrophobic backgrounds in the absence of serum or adsorbed proteins.¹¹⁻¹³ Under similar conditions (Fig. 6), we observed that cell attachment was significantly higher to quaternary amine surfaces relative to all others tested. Cell attachment to quaternary amine surfaces was over 400% greater than to amine surfaces, suggesting that in protein-free conditions, positively charged surface functional groups play a much more important role in promoting cell attachment. Massia and Hubbell have demonstrated that cell attachment to positively charged amine surfaces is inhibited by chondroitinase ABC, suggesting that electrostatic interactions between positively charged surface groups and negatively charged chondroitin sulfate proteoglycans are important in the mechanism of cell adhesion to positively charged surfaces without the presence of adsorbed proteins.²² In our experiments, oxidized thiol surfaces achieved the lowest level of cell attachment, suggesting that this negatively charged surface electrostatically may inhibit interactions with cell surface proteoglycans or prevent adsorption of adhesive proteins (Fig. 6).

Enhanced cell spreading on hydrophilic surfaces relative to hydrophobic surfaces has been observed by many researchers.^{16,23-25} Our results extend these observations by studying cell spreading, shape, and cytoskeletal organization over a range of surface wettability and charge. In our experiments, cells exhibited two primary morphologies, one rounded with high cell area, numerous highly organized actin stress fibers, and numerous focal adhesions, and a second

morphology characterized by a bipolar shape with reduced cell area, minimal actin stress fibers, and fewer focal adhesions that were localized primarily to one region of the cell periphery. Although examples of both morphologies were present on all surfaces, the rounded, well spread morphology was predominant on hydrophilic surfaces while the bipolar morphology predominated on hydrophobic surfaces. Among the three hydrophilic surfaces, the degree of wettability and differences in charged functional groups did not significantly affect cell area or cell shape as characterized by aspect ratio. However, between the two hydrophobic surfaces, the difference in wettability did result in a significant change in cell area but not in cell shape. Although cytoskeletal organization was not quantified, these results appear to depend only on general hydrophilicity or hydrophobicity, with little difference observed among the surfaces in each category. Several other groups have made similar observations of enhanced cytoskeletal organization on hydrophilic versus hydrophobic surfaces.^{25,26}

The greater number of adherent cells on thiol surfaces preadsorbed with the specific cell binding proteins fibronectin and laminin probably resulted from a higher concentration of adsorbed protein on the thiol surface. Oxidized thiol surfaces have been shown to reduce protein adsorption by as much as 70% relative to thiol surfaces.²⁷ Similarly, Clark et al. have demonstrated greater laminin adsorption and cell attachment on hydrophobic silanes patterned on plain glass.²⁸

Finally, the preadsorption of our model surfaces with BSA produced a pattern of cell attachment similar to that observed following 5% serum preadsorption. BSA was effective particularly at reducing or eliminating cell adhesion to the hydrophobic thiol and methyl surfaces. Williams et al. reported similar results using methyl-silica gradient surfaces where BSA preadsorption completely eliminated cell attachment to the hydrophobic end of the gradient.²⁹ Although a thicker layer of adsorbed BSA was present on the hydrophobic end of the gradient, this protein retained very little antialbumin binding activity, suggesting the protein was largely denatured. Ranieri et al. also have observed loss of cell attachment to hydrophobic fluorinated polymers preadsorbed with BSA.³⁰

One of the primary challenges in developing tissue-engineered devices is culturing anchorage-dependent cell populations on synthetic materials while maintaining their differentiated properties and functions. Several recent studies have suggested that cell spreading, shape, and cytoskeletal organization have a significant influence on cell differentiation. Ben-Ze'ev et al. found that primary hepatocytes seeded on dried rat tail collagen attained a flat, well spread morphology accompanied by high levels of DNA synthesis, high levels of mRNAs for cytoskeletal proteins, and low levels of mRNAs for liver-specific proteins.³¹ However, when these cells were plated on Engelbreth-Holm-Swarm (EHS) matrix, they assumed a small, spherical shape with reduced levels of DNA synthesis, reduced cytoskeletal mRNAs, and higher expression of mRNAs for liver-specific proteins. Using photolithographic methods to control cell area, Singhvi et al. demonstrated that hepatocyte production of albumin is greater when cells are restricted to a minimal spread area relative to well spread cells on unpatterned surfaces.³² Similarly, proper three-dimensional shape and multicellular organization is necessary for the production of whey acidic proteins from differentiated primary mammary epithelial cells.³³

The protein composition at a cell material interface can profoundly influence gene expression and cell differentiation. For example, fibronectin has been shown to play an important role in preventing the premature differentiation of immature, rapidly proliferating keratinocytes at the epithelial basal lamina.³⁴ Similarly, laminin can stimulate β -casein production by mammary epithelial cells in a concentration-dependent manner through integrin binding.³⁵ When adsorbed to plastic surfaces, fibronectin and type IV collagen stimulate distinct patterns of cytokine gene expression in macrophages.³⁶

In order to engineer material surfaces with optimal properties for maintaining cell differentiation, one must understand the complex interrelationships among material surface properties, adsorbed proteins, and cellular responses. In summary, our results suggest that serum-treated hydrophilic surfaces support significantly greater cell attachment, cell spreading, and cytoskeletal organization relative to hydrophobic surfaces. Among hydrophilic surfaces, differences in wettability and charged functional groups significantly influence cell attachment but not spreading or cytoskeletal organization. Moderate surface wettability is the major factor promoting high levels of cell attachment to serum-treated hydrophilic surfaces, with a smaller contribution due to positively charged functional groups. However, in protein-free conditions, the presence of positively charged functional groups is the primary factor promoting increased cell attachment. Our studies with individual proteins suggest that BSA plays an important role in regulating cell attachment, particularly on hydrophobic surfaces. Future studies will extend this work by exploring how longer-term cellular responses, such as cell proliferation, migration, and differentiation, are influenced by modified surfaces with different functional groups and adsorbed proteins.

Acknowledgements

Contract grant sponsor: Center for Biopolymers at Interfaces, University of Utah

Contract grant sponsor: Whitaker Foundation grant to Biobased Engineering Program, Department of Bioengineering, University of Utah

References

- Burridge K, Fath K, Kelly T, Nuckolls G, Turner C. Focal adhesions: Transmembrane junctions between the extracellular matrix and the cytoskeleton. *Ann. Rev. Cell Biol* 1988;4:487–525. [PubMed: 3058164]
- Clark EA, Brugge JS. Integrins and signal transduction pathways: The road taken. *Science* 1995;268:233–239. [PubMed: 7716514]
- Miyamoto S, Teramoto H, Coso OA, Gutkind JS, Burbelo PD, Akiyama SK, Yamada KM. Integrin function: Molecular hierarchies of cytoskeletal and signaling molecules. *J. Cell Biol* 1995;131:791–805. [PubMed: 7593197]
- Schwartz MA, Schaller MD, Ginsberg MH. Integrins: Emerging paradigms of signal transduction. *Ann. Rev. Cell Dev. Biol* 1995;11:549–599. [PubMed: 8689569]
- Andrade JD, Hlady V. Protein adsorption and materials biocompatibility: A tutorial review and suggested hypotheses. *Adv. Polym. Sci* 1986;79:1–63.
- Kleinfeld D, Kahler KH, Hockberger PE. Controlled outgrowth of dissociated neurons on patterned substrates. *J. Neurosci* 1988;8:4098–4120. [PubMed: 3054009]
- Dulcey CS, Georger JH, Krauthamer V, Stenger DA, Fare TL, Calvert JM. Deep UV photochemistry of chemisorbed monolayers: Patterned coplanar molecular assemblies. *Science* 1991;252:551–555. [PubMed: 2020853]
- Georger JH, Stenger DA, Rudolph AS, Hickman JJ, Dulcey CS, Fare TL. Coplanar patterns of self-assembled monolayers for selective cell adhesion and outgrowth. *Thin Solid Films* 1992;210:716–719.
- Stenger DA, Georger JH, Dulcey CS, Hickman JJ, Rudolph AS, Nielsen TB, McCort SM, Calvert JM. Coplanar molecular assemblies of amino- and perfluorinated alkylsilanes: Characterization and geometric definition of mammalian cell adhesion and growth. *J. Am. Chem. Soc* 1992;114:8435–8442.
- Britland S, Clark P, Connolly P, Moores G. Micropatterned substratum adhesiveness: A model for morphogenetic cues controlling cell behavior. *Exp. Cell Res* 1992;198:124–129. [PubMed: 1727046]
- Matsuzawa M, Potember RS, Stenger DA, Krauthamer V. Containment and growth of neuroblastoma cells on chemically patterned surfaces. *J. Neurosci. Meth* 1993;50:253–260.
- Lom B, Healy KE, Hockberger PE. A versatile technique for patterning biomolecules onto glass coverslips. *J. Neurosci. Meth* 1993;50:385–397.

13. Healy KE, Lom B, Hockberger PE. Spatial distribution of mammalian cells dictated by material surface chemistry. *Biotechnol. Bioeng* 1994;43:792–800. [PubMed: 18615803]
14. Healy KE, Thomas CH, Rezania A, Kim JE, Mc-Keown PJ, Lom B, Hockberger PE. Kinetics of bone cell organization and mineralization on materials with patterned surface chemistry. *Biomaterials* 1996;17:195–208. [PubMed: 8624396]
15. Clark P, Moores GR. Cell guidance by micropatterned adhesiveness *in vitro*. *J. Cell Sci* 1992;103:287–292. [PubMed: 1429909]
16. Ruardy TG, Schakenraad JM, van der Mei HC, Busscher HJ. Adhesion and spreading of human skin fibroblasts on physicochemically characterized gradient surfaces. *J. Biomed. Mater. Res* 1995;29:1415–1423. [PubMed: 8582910]
17. Liu J, Hlady V. Chemical pattern on silica surface prepared by UV irradiation of 3-mercaptopropyltriethoxy silane layer: Surface characterization and fibrinogen adsorption. *Coll. Surfaces B: Biointerfaces* 1996;8:25–37.
18. Bhatia SK, Hickman JJ, Ligler FS. New approach to producing patterned biomolecular assemblies. *J. Am. Chem. Soc* 1992;114:4432–4433.
19. Balachander N, Sukenik CN. Monolayer transformation by nucleophilic substitution: Applications to the creation of new monolayer assemblies. *Langmuir* 1990;6:1621–1627.
20. van Wachem PB, Beugeling T, Feijen J, Bantjes A, Detmers JP, van Aken WG. Interaction of cultured human endothelial cells with polymeric surfaces of different wettabilities. *Biomaterials* 1985;6:403–408. [PubMed: 4084642]
21. van Wachem PB, Hogt AH, Beugeling T, Feijen J, Bantjes A, Detmers JP, van Aken WG. Adhesion of cultured human endothelial cells onto methacrylate polymers with varying surface wettability and charge. *Biomaterials* 1987;8:323–328. [PubMed: 3676418]
22. Massia SP, Hubbell JA. Immobilized amines and basic amino acids as mimetic heparin-binding domains for cell surface proteoglycan-mediated adhesion. *J. Biol. Chem* 1992;267:10133–10141. [PubMed: 1577783]
23. van der Valk P, van Pelt AWJ, Busscher HJ, de Jong HP, Wildevuur CRH, Arends J. Interaction of fibroblasts and polymer surfaces: Relationship between surface free energy and fibroblast spreading. *J. Biomed. Mater. Res* 1983;17:807–817. [PubMed: 6619177]
24. Schakenraad JM, Busscher HJ, Wildevuur CRH, Arends J. The influence of substratum surface free energy on growth and spreading of human fibroblasts in the presence and absence of serum proteins. *J. Biomed. Mater. Res* 1986;20:773–784. [PubMed: 3722214]
25. Juliano DJ, Saavedra SS, Truskey GA. Effect of the conformation and orientation of adsorbed fibronectin on endothelial cell spreading and the strength of adhesion. *J. Biomed. Mater. Res* 1993;27:1103–1113. [PubMed: 8408123]
26. Altankov G, Grinnell F, Groth T. Studies on the biocompatibility of materials: Fibroblast reorganization of sub-stratum-bound fibronectin on surfaces varying in wettability. *J. Biomed. Mater. Res* 1996;30:385–391. [PubMed: 8698702]
27. Bhatia SK, Teixeira JL, Anderson M, Shriver-Lake LC, Calvert JM, Georger JH, Hickman JJ, Dulcey CS, Schoen PE, Ligler FS. Fabrication of surfaces resistant to protein adsorption and application to two-dimensional protein patterning. *Anal. Biochem* 1993;208:197–205. [PubMed: 8434788]
28. Clark P, Britland S, Connolly P. Growth cone guidance and neuron morphology on micropatterned laminin surfaces. *J. Cell Sci* 1993;105:203–212. [PubMed: 8360274]
29. Williams RL, Hunt JA, Tengvall P. Fibroblast adhesion onto methyl-silica gradients with and without preadsorbed protein. *J. Biomed. Mater. Res* 1995;29:1545–1555. [PubMed: 8600145]
30. Ranieri JP, Bellamkonda R, Jacob J, Bargo TG, Gardella JA, Aebischer P. Selective neuronal cell attachment to a covalently patterned monoamine on fluorinated ethylene propylene films. *J. Biomed. Mater. Res* 1993;27:917–925. [PubMed: 8360219]
31. Ben-Ze'ev A, Robinson GS, Bucher NLR, Farmer SR. Cell-cell and cell-matrix interactions differentially regulate the expression of hepatic and cytoskeletal genes in primary cultures of rat hepatocytes. *Proc. Natl. Acad. Sci. USA* 1988;85:2161–2165. [PubMed: 3353374]
32. Singhvi R, Kumar A, Lopez GP, Stephanopoulos GN, Wang DIC, Whitesides GM, Ingber DE. Engineering cell shape and function. *Science* 1994;264:696–698. [PubMed: 8171320]

33. Chen LH, Bissell MJ. A novel regulatory mechanism for whey acidic protein gene expression. *Cell Reg* 1989;1:45–54.
34. Adams JC, Watt FM. Fibronectin inhibits the terminal differentiation of human keratinocytes. *Nature* 1989;340:307–309. [PubMed: 2473404]
35. Streuli CH, Schmidhauser C, Bailey N, Yurchenco P, Skubitz APN, Roskelley C, Bissell MJ. Laminin mediates tissue-specific gene expression in mammary epithelia. *J. Cell Biol* 1995;129:591–603. [PubMed: 7730398]
36. Eierman DF, Johnson CE, Haskill JS. Human monocyte inflammatory mediator gene expression is selectively regulated by adherence substrates. *J. Immunol* 1989;142:1970–1976. [PubMed: 2784145]

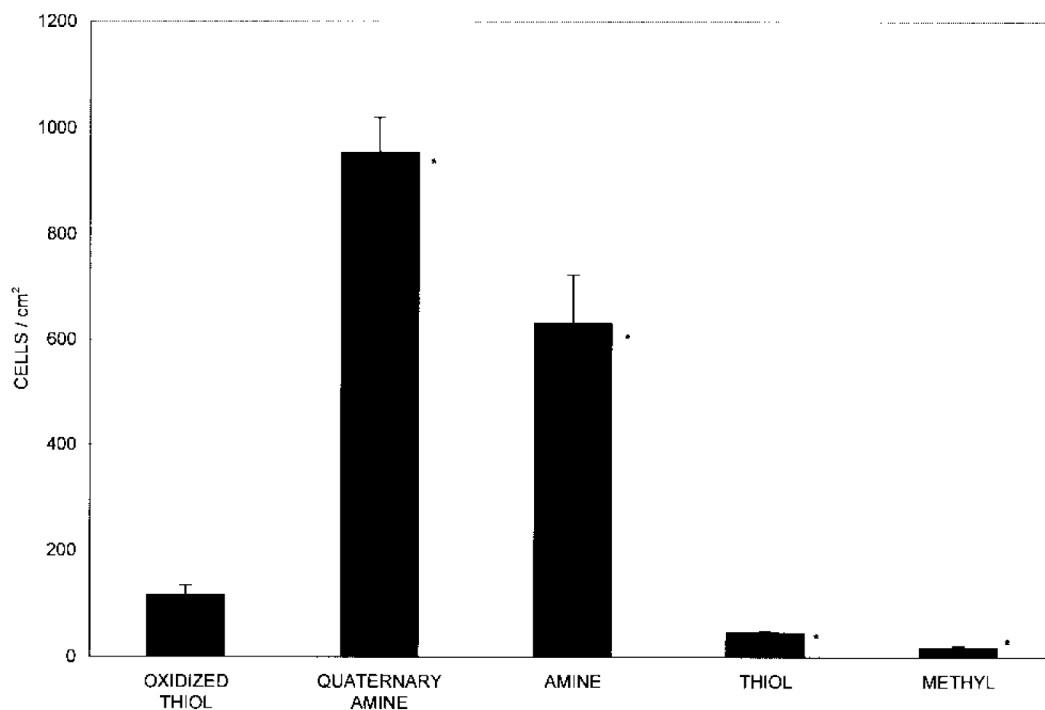


Figure 1. NIH 3T3 fibroblast attachment to model surfaces preadsorbed with 5% serum. Model surfaces are listed along the x axis in order of increasing hydrophobicity as determined by static water contact angle. $N = 6$ surfaces; * = $p < 0.05$ relative to oxidized thiol.

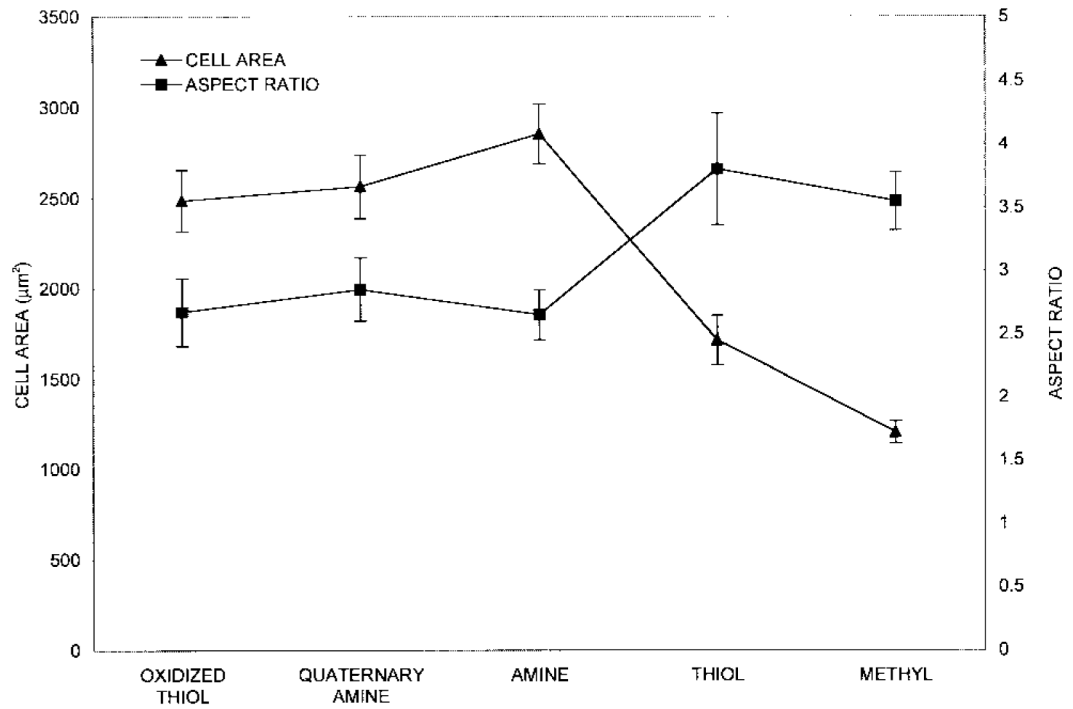


Figure 2. NIH 3T3 fibroblast area and aspect ratio on model surfaces preadsorbed with 5% serum. $N = 3$ surfaces with 21 cells analyzed per surface.

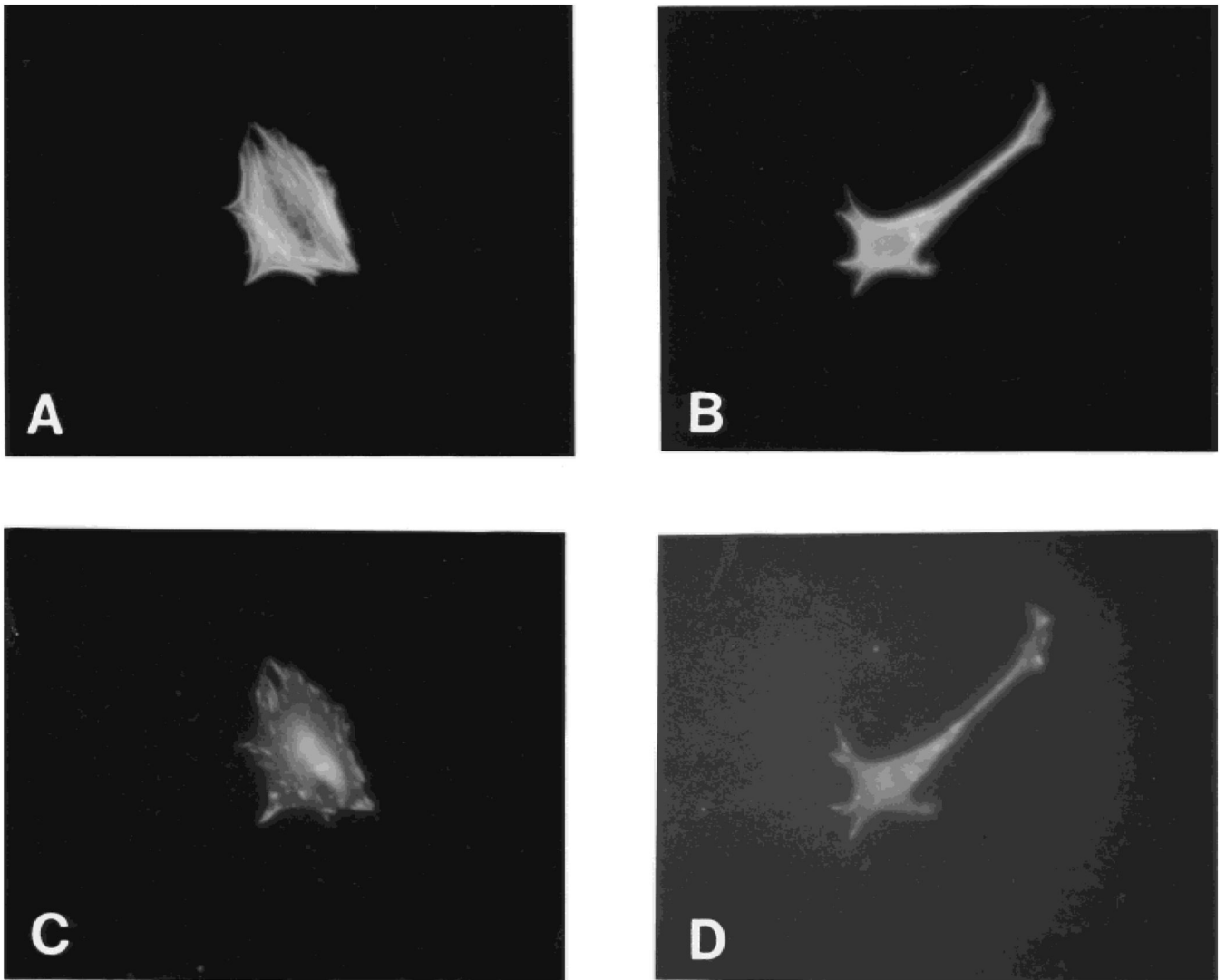


Figure 3. Cytoskeletal organization of NIH 3T3 fibroblasts representative of the predominant morphologies on oxidized thiol, quaternary amine, and amine surfaces (a,c) and thiol and methyl surfaces (b,d). Cells were stained with rhodamine-phalloidin for actin (a,b) and by indirect immunofluorescence for vinculin (c,d). Original magnification 400 \times .

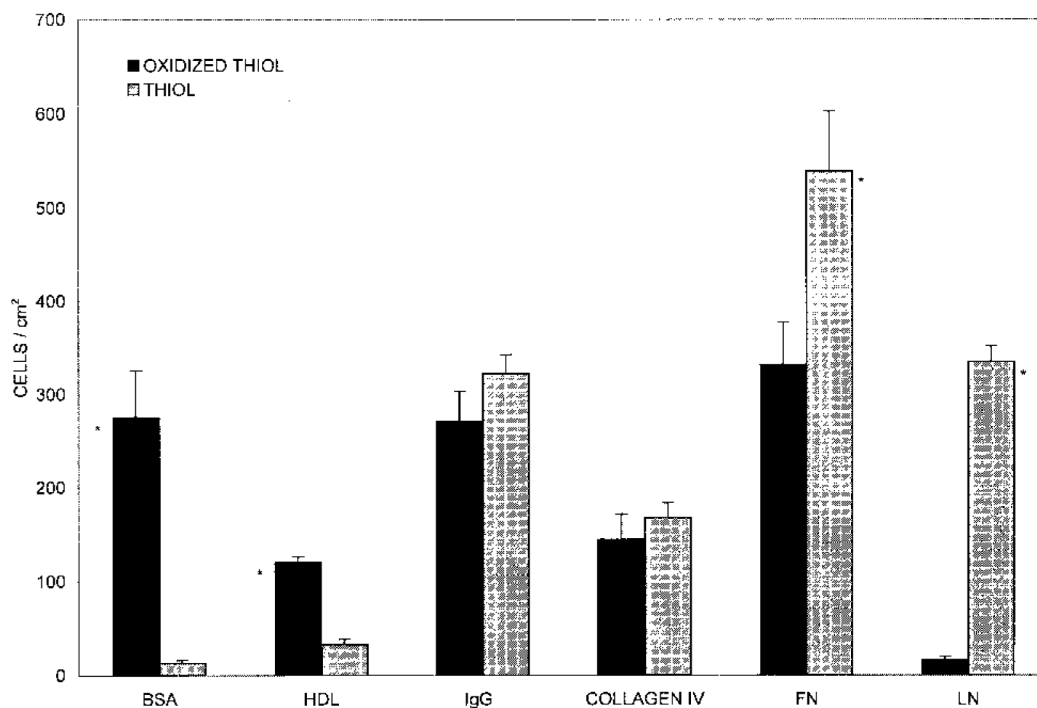


Figure 4. NIH 3T3 fibroblast attachment to oxidized thiol/thiol surfaces preadsorbed with bovine serum albumin (BSA, 2.1 mg/mL), high density lipoprotein (HDL, 65 μ g/mL), immunoglobulin G (IgG, 0.5 mg/mL), type IV collagen (33 μ g/mL), fibronectin (FN, 20 μ g/mL), and lamina (LN, 20 μ g/mL). $N = 3$ surfaces. * = $P < 0.05$.

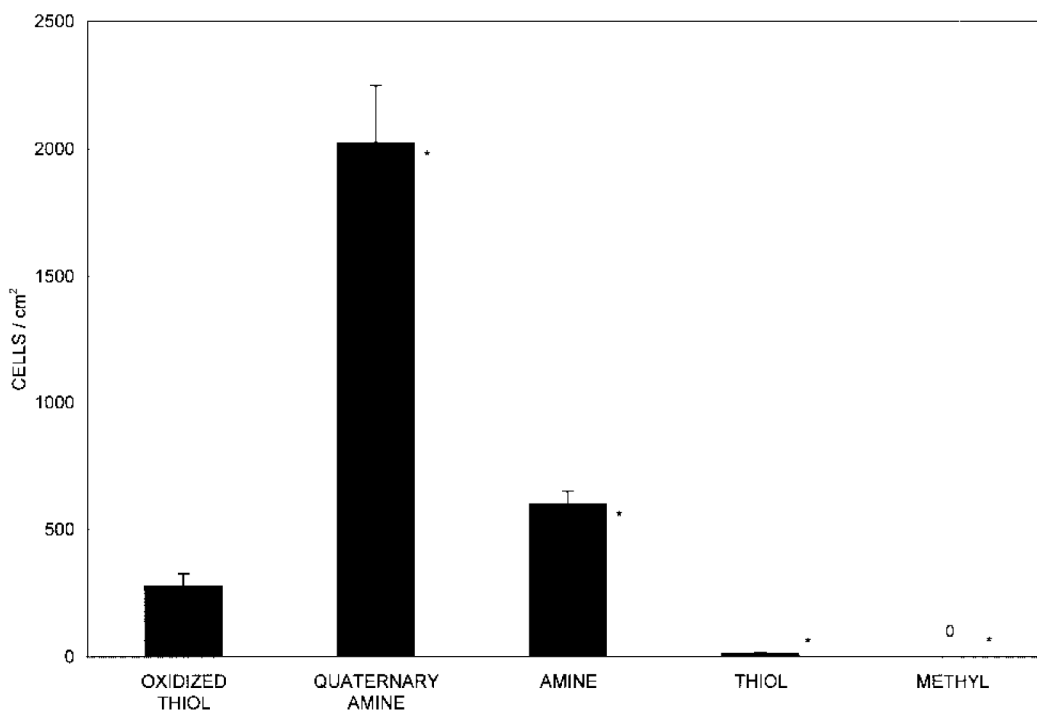


Figure 5. NIH 3T3 fibroblast attachment to model surfaces preadsorbed with 2.1 mg/mL of BSA. $N = 3$ surfaces. * = $P < 0.05$ relative to oxidized thiol.

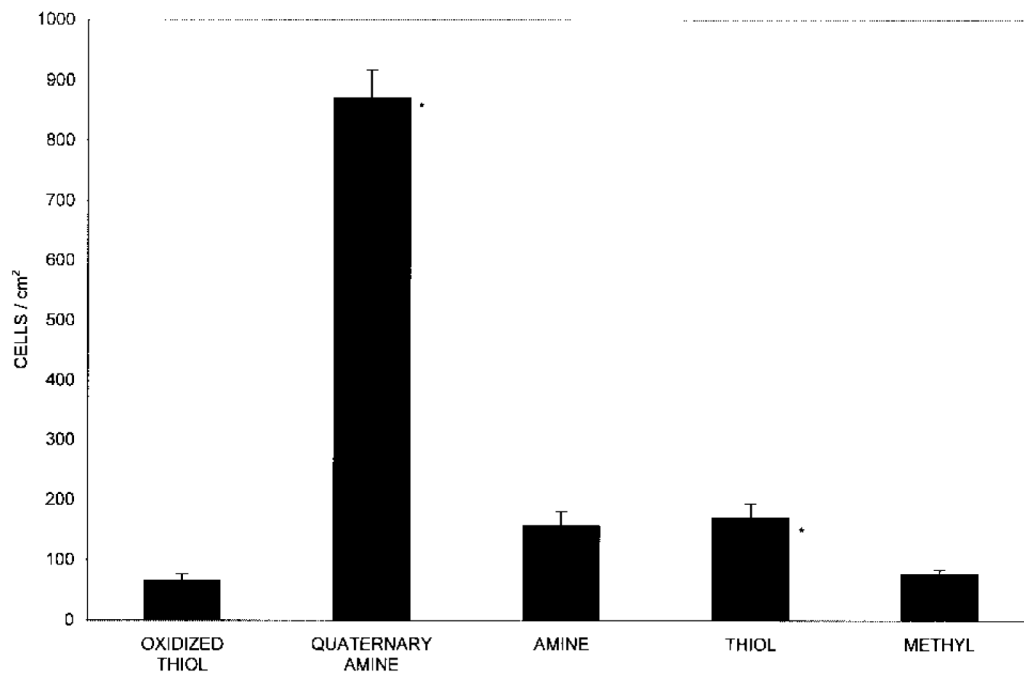


Figure 6.

NIH 3T3 fibroblast attachment to model surfaces without preadsorbed protein. $N = 3$ surfaces.

* = $P < 0.05$ relative to oxidized thiol.

TABLE I
Water Contact Angles and Atomic Composition of Modified Glass Surfaces

Surface Chemistry	Contact Angle		C	N	O	S	XPS Atomic Percent Values	
	pH 2.0	pH 7.5					Si	P
Clean glass	wetting	wetting	6.4		60.2		33.4	
Oxidized	ND	7.3 ± 0.5	15.5		52.4	3.2	28.8	
thiol								
Quaternary amine	21.6 ± 0.5	22.7 ± 0.6	ND	ND	ND	ND	ND	ND
Amine	20.1 ± 0.5	36.7 ± 0.6	9.7	1.7	56.6		32.0	
Thiol	ND	59.7 ± 0.6	14.8		49.4	3.9	31.9	
Methyl	ND	92.0 ± 0.6	11.7		54.6		33.7	

Static water contact angles were measured by the sessile drop method at ambient temperature. Distilled water buffered with 1.45 mM of sodium phosphate monobasic and 8.1 mM of sodium phosphate dibasic and titrated to pH 2.0 and 7.5 was used as the probe liquid. Clean glass was completely wetting. Data are expressed as mean ± standard error of mean ($n = 7$). Atomic percent values were calculated from XPS data. ND = not determined.